

Thorium adsorption by oxidized biochar pine needles - The effect of particle size

K. Philippou¹, A. Konstantinou¹, I. Pashalidis¹

¹Department of Chemistry, University of Cyprus, P.O. Box 20537, Cy-1678 Nicosia, Cyprus

Keywords: Oxidized biochar pine needles, Th(IV), adsorption, particle size, aqueous solutions

Presenting author email: kphili03@ucy.ac.cy

Abstract

Removal and recovery of economically important (radio)toxic metals from industrial process and waste waters is of particular interest in the frame of environmental protection and the need to cover the growing demand on sustainable energy production. Thorium (Th-232) is a potential primary fuel in nuclear industry it can be used in different reactor types and has compared to uranium important waste disposal and proliferation advantages. The present study deals with adsorption/removal of Th(IV) from aqueous solutions and particularly the effect of particle size on the metal ion adsorption by oxidized biochar fibres derived from pine needles. The adsorption experiments were performed by batch-type experiments and include the effect of particle size on the adsorption capacity (q_{\max}) and adsorption kinetics (k_1), as well as FTIR studies and XRD measurements for the characterization of adsorbed species and solid phases, respectively. The experimental data indicate that there is an optimum range of particle size in which the maximum values for the adsorption capacity ($q_{\max}= 0.76 \text{ mol kg}^{-1}$ or 181 g kg^{-1}) and the kinetic constant ($k_1= 0.3 \text{ s}^{-1}$) are observed.

Introduction

Removal and recovery of economically important metals from industrial process and waste waters is of particular interest in the frame of environmental protection and the need to cover the growing demand for metals that play a key role in green and sustainable energy production and manufacturing [1, 2]. Various techniques have been developed to remove (radio)toxic metals from contaminated waters, including chemical oxidation, electrocoagulation, solvent extraction and adsorption [1, 2]. Amongst the various techniques that have been developed for the recovery of metal ions from aqueous systems, adsorption and specifically biosorption is the method of choice for wastewater remediation and metal-ion recovery due to its simplicity, low cost and efficiency [1-3]. The last decade, there is increased interest in the use of biochar fibers, which present remarkable adsorbent properties, such as easy material transport and high external surface available for adsorption. In addition, their affinity can be enhanced towards hard metal ions after oxidation and the formation of surface carboxylic moieties [4-7].

The present study is focused on thorium (Th) because this actinide is a potential primary fuel in nuclear industry and can be used as alternative to uranium (U-235), because of its important waste disposal and proliferation advantages [8]. Hence, anthropogenic activities related to thorium fuel cycle, which are associated with large volumes of process and waste waters containing thorium, could result in environmental pollution in the near field of such activities [9]. The experiments have been carried out with Th(IV) because tetravalent thorium (Th(IV)) is the predominant oxidation state in aqueous systems [7, 10]. There are few studies related to Th(IV) adsorption by biochar fibers, which have been focused on the effect of various physicochemical parameters (e.g. pH, metal ion concentration, temperature, contact time, ionic strength) affecting the adsorption efficiency [7, 12, 13]. However, to the best of our knowledge, there are no investigations dealing with the effect of biochar particle size on the adsorption efficiency. Hence the present study deals with the adsorption of Th(IV) from aqueous solutions and in particular with the effect of particle size on the adsorption efficiency of thorium by oxidized biochar fibres derived from pine needles (pnco).

Experimental

The adsorption experiments and the determination of thorium concentration in the test solutions were carried out as described elsewhere [7, 12, 14]. The adsorbent used was oxidized biochar prepared from pine needles. The pine needles were collected from locally grown pine tree (*Pinus brutia Pegeia*). The washed and air-dried needles were thermally treated under anoxic conditions (N₂) to obtain the carbonized product. The biochar was then oxidized with concentrated nitric acid (8 M HNO₃, 3h) and prepared for the characterization studies (FTIR, XRD, acid-base titration) as described elsewhere [7, 12, 14]. The different biochar particle fractions were obtained by using sieves of different mesh sizes (> 500 μm, 500 μm - 200 μm, 200 μm - 100 μm, 100 μm – 50 μm and < 50 μm).

Thorium adsorption on the oxidized biochar was investigated by batch equilibrium experiments as described elsewhere [7, 12] at pH 3, constant mass of the biochar (m= 0.01 g) and variable initial metal ion concentration ($5 \times 10^{-6} \text{ mol L}^{-1} < [\text{Th(IV)}] < 5 \times 10^{-3} \text{ mol L}^{-1}$, at pH 3). For the kinetic experiments pH, initial metal ion concentration and mass of the biochar were kept constant and the contact time was between 0 and 1440 minutes). The data analysis, as well as the uncertainty evaluation, were carried out as described elsewhere [7, 14]. The relative amount of metal ion adsorbed was determined using the following equations:

$$(\%) \text{ rel. adsorption} = 100 \times \frac{([\text{Th(IV)}]_0 - [\text{Th(IV)}]_{aq})}{[\text{Th(IV)}]_0} \quad (1)$$

where $[\text{Th(IV)}]_o$ = the total metal ion concentration ($\text{mol}\cdot\text{l}^{-1}$) in the system or in the reference solution, $[\text{Th(IV)}]_{\text{aq}}$ = metal ion concentration ($\text{mol}\cdot\text{l}^{-1}$) in the test solution. In addition, $[\text{Th(IV)}]_{\text{aq}}$ is equal to C_e ($\text{mol}\cdot\text{l}^{-1}$) and q corresponds to the amount of $M(z)$ adsorbed per unit mass of adsorbent.

The effect of temperature and contact time in order to evaluate the thermodynamic and kinetic parameters ΔH° and ΔS° , and k_1 , respectively, was carried out using 30 mL aqueous solutions containing 0.01 g of the adsorbent and 5×10^{-4} M Th(IV) at pH 3. Evaluation of the thermodynamic parameters was performed using equations (3) and (4):

$$\ln K_d = -\frac{\Delta H^\circ}{RT} + \frac{\Delta S^\circ}{R} \quad (3)$$

and

$$K_d = \frac{([\text{Th(IV)}]_o - [\text{Th(IV)}]_e) \cdot \frac{V}{m}}{[\text{Th(IV)}]_e} \quad (4)$$

where K_d is the distribution coefficient, ΔH° and ΔS° the standard enthalpy and entropy, respectively, T the temperature in K, R is the universal gas constant, V the solution volume and m the mass of the adsorbent.

The adsorption experimental data have been fitted using the *Langmuir* isotherm. The *Langmuir* isotherm model is based on the assumption that all surface sites are similar and independent of their neighbouring sites occupancy. Since, Th(IV) adsorption is expected to take place on specific surface active groups (e.g. carboxylic groups) forming inner-sphere complexes [7, 12], the *Langmuir* isotherm model is expected to fit well the experimental data. Moreover, the maximum adsorption capacity q_{max} is expected to coincide with the maximum number of surface sites available for adsorption. The *Langmuir* isotherm model can be described by equation 5:

$$q_{\text{max}} = \frac{q_{\text{max}} \times K_L \times C_e}{1 + K_L \times C_e} \quad (5)$$

where q_{max} is the maximum monolayer adsorption capacity (mg g^{-1}) and K_L is the *Langmuir* isotherm constant (L mg^{-1}) related to adsorption energy [15, 16].

Results and Discussion

Th(IV) adsorption by oxidized pine needle biochar (pnco)

The adsorption of Th(IV) by oxidized biochar fibers have been previously investigated using oxidized biochar fibers obtained from opuntia ficus indica and luffa cylindrical plant fibers [7, 12]. The adsorption experiments, which have been performed at pH 3 to avoid hydrolysis reactions and the formation of Th(IV) colloidal species and Th(OH)₂ surface precipitation, and the resulting data have shown increased adsorption of thorium, which was ascribed to the formation of inner-sphere complexes between Th(IV) and the carboxylic groups present on the biochar surface [7, 12]. Similarly, interaction of Th(IV) with oxidized pine needle biochar (pnco) results in the formation of inner-sphere complexes as indicated by the corresponding IR spectra in figure 1. The peak at 3443 cm⁻¹ and 1705 cm⁻¹ are attributed the stretching vibrations of O-H associated with the carboxylic moieties or the adsorbed water and the carboxylic moiety (C=O), respectively. The peak at 1630 cm⁻¹ corresponds to the bending vibrations of adsorbed water molecules, whereas the peak at 1611 cm⁻¹ to the stretching vibrations the carboxylic C-O moiety ν (C-O). Moreover, the peaks observed at 1369 cm⁻¹, 1241 cm⁻¹, 1098 cm⁻¹ and 614 cm⁻¹ are observed due to the bending vibrations of C-O and C-H groups, respectively [7, 12].

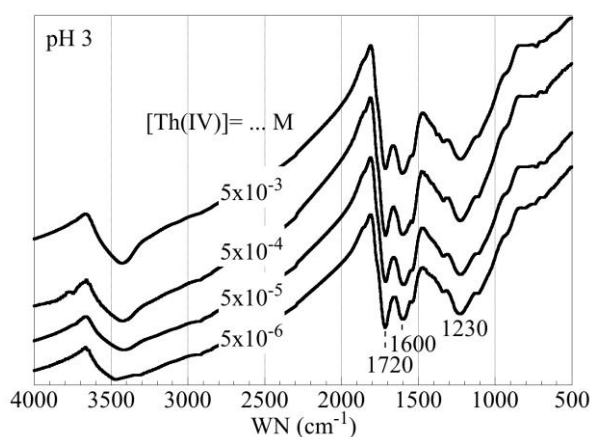
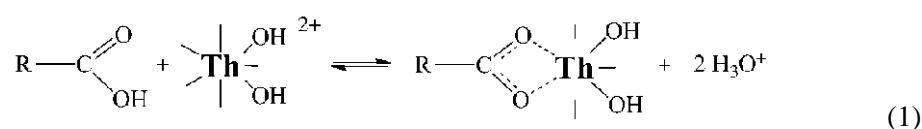


Fig. 1 FTIR spectra of the oxidized biochar after Th(IV) adsorption at pH 3.0 and at different thorium concentrations

The significant changes in the peak ratio at 1705 and 1611 cm⁻¹ with increasing initial metal concentration indicates the formation of inner-sphere surface complexes between Th(IV) and the surface carboxylic moieties as schematically described by Eq. (1):



The Th(IV) adsorption is expected to occur via cation exchange reactions, as described by Eq. (1), because at pH 3 the carboxylic moieties are protonated and Th(IV) is expected to be present as di-hydroxy complex [10].

Effect of particle size on the adsorption capacity

The adsorption capacity of the oxidized biochar regarding Th(IV) adsorption has been investigated as a function of the pncO particle size by batch-type equilibrium experiments. The related experimental data are shown in Fig. 2 and indicate that the pncO fraction with particle size between 100 μm and 200 μm presents significantly higher adsorption capacity than the other fractions. This could be attributed to the fact at this particle fraction the oxidized biochar offers the highest surface available for adsorption since the particles are small enough but do not stick with one another, resulting in lower specific surface area.

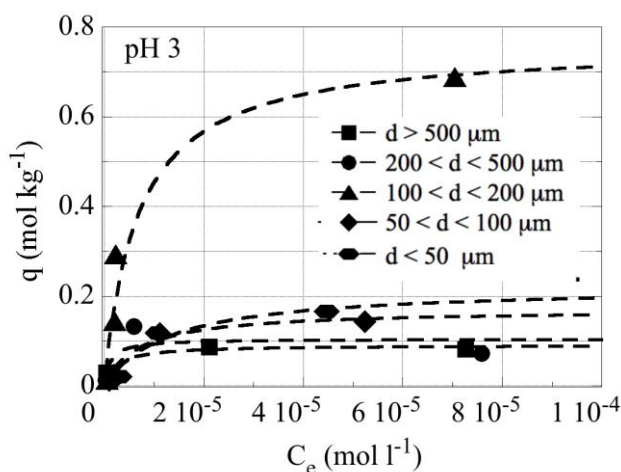


Fig. 2 Adsorption isotherms of Th(IV) adsorption on oxidized pine needle biochar (pncO) as a function of the biochar particle size at pH 3 (0.01 g of biochar, $V = 30$ mL, $[\text{Th(IV)}]_0 = 5 \times 10^{-6} - 5 \times 10^{-3}$ mol L^{-1} , $T = 23 \pm 2^\circ\text{C}$, 3 days reaction time)

The evaluation of the maximum adsorption capacities (q_{max}) has been carried out by applying the *Langmuir* adsorption isotherm model to the experimental data and the q_{max} values obtained are summarized in Table 1.

Table 1: Maximum adsorption capacities (q_{max}) for the Th(IV) adsorption by pncO as function of the particle size fraction

Particle fraction	q_{max}	R
-------------------	------------------	---

> 500	0.09	0.94
500 - 200	0.10	0.79
200 - 100	0.76	0.97
100 – 50	0.17	0.98
< 50	0.22	0.98

The q_{\max} value of the biochar fraction between 100 μm and 200 μm is generally higher than q_{\max} values found in literature for Th(IV) adsorption by biomasses and carbonaceous materials [7, 12, 13, 17-22], especially under such an acidic environment (Table 2).

Table 2 Comparison of adsorption capacities values (q_{\max}) of various adsorbent materials for Th(IV).

Adsorbent	pH	q_{\max} (mg g ⁻¹)	References
Activated carbon from olive stone	4	20.19	[17]
Nano-iron oxide (Fe ₂ O ₃)-impregnated cellulose acetate composite	6	21.3	[18]
<i>Cystoseira indica</i> alga	3.5	195.7	[19]
CaCl ₂ -modified <i>Giant Kelp</i> biomass	3.5	135	[20]
Graphene oxide	2.9	134.58	[21]
Activated biochar fibres derived from <i>Opuntia Ficus Indica</i>	3	81	[12]
Reduced graphene oxide	3	48.73	[22]
Oxidized biochar fibres derived from <i>Luffa cylindrical</i>	3	70	[7]
NaOH-modified biomass derived from <i>duckweed</i>	3	96.3	[13]
Oxidized biochar fibres derived from <i>pine needles</i>	3	181	Present study

In order to prove that no surface precipitation has occurred, XRD measurements have been performed and the corresponding diffractograms are presented in Fig. 3. According to Fig. 3 only the graphite peaks are observed and there is no indication of Th(IV) solid phase precipitation up to thorium concentration of 5×10^{-3} mol L⁻¹, at pH 3.

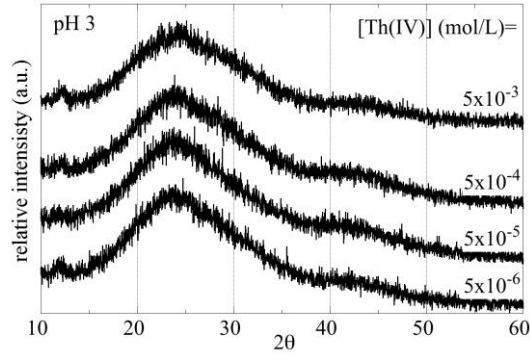


Fig. 3 XRD spectra of the oxidized biochar after Th(IV) adsorption at pH 3 and at different thorium concentrations

Effect of pnco particle size on the adsorption kinetics

The adsorption of Th(IV) by oxidized biochar fibers is a relatively fast two step process (Fig. 4), whereby the first step corresponds to the interaction of the Th(IV) cations with the surface carboxylic moieties and the second step the metal ion diffusion within the biochar channels [7, 12].

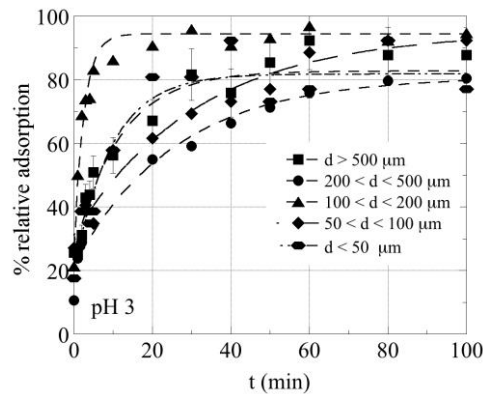


Fig. 4 Relative adsorption of Th(IV) by oxidized pine needle biochar as a function of time and for different biochar fractions at pH 3 (0.03 g of biochar, $V = 100$ mL, $[\text{Th(IV)}]_0 = 5 \times 10^{-4}$ mol L⁻¹, $T = 23 \pm 2$ °C, 24 h reaction time)

In order to evaluate the adsorption kinetics of the present system the *Lagergren* pseudo-first order model has been applied to the experimental data corresponding to the first fast adsorption step and obtained using biochar samples of different particle fraction [7, 12]. The respective graphs are shown in Fig. 5, and the evaluated data are summarized in Table 3. The kinetic constant (k_1) was calculated using the *Lagergren* equation (Eq. (6)):

$$\ln(q_e - q_t) = \ln q_e - k_1 t \quad (6)$$

where q_e is the adsorbed amount of the metal ion in equilibrium (mol kg^{-1}), q_t is the adsorbed amount of the metal ion at time t (mol kg^{-1}), k_1 is the kinetic constant of the pseudo-first order kinetic model (min^{-1}) and t is the time (min).

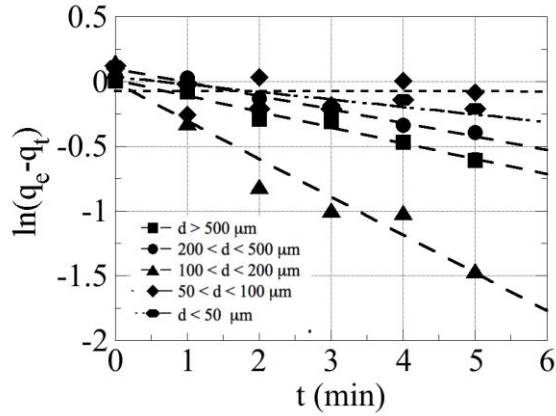


Fig. 5 Lagergren plots corresponding to Th(IV) adsorption on oxidized pine needle biochar (pmco) as a function of the biochar particle size at pH 3 (0.03 g of biochar, $V = 100 \text{ mL}$, $[\text{Th(IV)}]_0 = 5 \times 10^{-4} \text{ mol L}^{-1}$, $T = 23 \pm 2 \text{ }^\circ\text{C}$, 24 h reaction time)

Table 3: Kinetic constants (k_1) for the Th(IV) adsorption by pmco as function of the particle size fraction

Particle fraction	k_1 (s^{-1})	R
> 500	0.12	0.99
500 – 200	0.11	0.99
200 – 100	0.30	0.97
100 – 50	0.01	0.79
< 50	0.05	0.80

Based on the experimental results summarized in Table 3, it is obvious that the particle size affects significantly the adsorption rate. Nevertheless, the values of the k_1 are in the range of corresponding values obtained from other thorium adsorption systems found in literature [12, 22].

Conclusion

The adsorption capacity of pncO for Th(IV) and the corresponding adsorption rates depend strongly on the biochar particle size. The optimum range of particle size in which the maximum values for the adsorption capacity ($q_{\max} = 0.76 \text{ mol kg}^{-1}$ or 181 g kg^{-1}) and the kinetic constant ($k_1 = 0.3 \text{ s}^{-1}$) are observed is between $200 - 100 \text{ }\mu\text{m}$. According to FTIR studies the adsorption occurs through the formation of inner-sphere complexes between Th(IV) and the carboxylic groups present on the biochar surface. Moreover, XRD measurements indicate that there is no surface precipitation of $\text{Th}(\text{OH})_4$ and the increased adsorption capacity is attributed to microchannels present in the pine needle biochar, which provide them large external surface available for adsorption.

References

1. Khalil, HPSA., Bhat, AH., Yusra, AFI.: Green composites from sustainable cellulose nanofibrils: a review. *Carbohydr. Polym.* 87, 963-979 (2012)
2. Michalak, I., Chojnacka, K., Witek-Krowiak, A.: State of the Art for the Biosorption Process—a Review. *Appl. Biochem. Biotechnol.* 170, 1389–1416 (2013)
3. Tarley, CRT., Arruda, MAZ.: Natural adsorbents: potential and applications of natural sponge (*Luffa cylindrica*) in lead removal in wastewater laboratory. *Revista Analytica.* 4, 26-31 (2003)
4. Liatsou, I., Constantinou, P., Pashalidis, I.: Copper binding by activated biochar fibres derived from *Luffa Cylindrica*. *Water Air Soil Poll.* (2017). doi: 10.1007/s11270-017-3411-8
5. Liatsou, I., Michail, G., Demetriou, M., Pashalidis, I.: Uranium binding by biochar fibres derived from *Luffa cylindrica* after controlled surface oxidation. *J Radioanal. Nucl. Ch.* 311, 871-875 (2017)
6. Hadjittofi, L., Prodromou, M., Pashalidis, I.: Activated biochar derived from cactus fibres – preparation, characterization and application on Cu(II) removal from aqueous solutions. *Bioresource Technol.* 159, 460-464 (2014)
7. Liatsou, I., Christodoulou, E., Pashalidis, I.: Thorium adsorption by oxidized biochar fibres derived from *Luffa cylindrica* sponges. *J Radioanal. Nucl. Ch.* 311, 871-875 (2018)
8. IAEA: Thorium fuel utilization: Options and trends. Proceedings of three IAEA meetings held in Vienna in 1997, 1998 and 1999. IAEA-TECDOC-1319 (2002)
9. Somayajulu, BLK., Goldberg, ED.: Thorium and Uranium Isotopes in Seawater and Sediments. *Earth Planet Sci. Lett.* 1, 102-106 (1966)

10. Fanghänel, Th., Neck, V.: Aquatic chemistry and solubility phenomena of actinide oxides/hydroxides. *Pure Appl. Chem.* 74, 1895-1907 (2002)
11. Metaxas, M., Kasselouri-Rigopoulou, V., Galiatsatou, P., Konstantopoulou, C., Oikonomou, D.: Thorium removal by different adsorbents. *J Hazard Mater.* B97, 71–82 (2003)
12. Hadjittofi, L., Pashalidis, I.: Thorium removal from acidic aqueous solutions by activated biochar derived from cactus fibers. *Desalin. Water Treat.* 57, 27864-27868 (2016)
13. Chen, T., Zhang, N., Xu, Z., Hu, X., Ding, Z.: Integrated comparisons of thorium(IV) adsorption onto alkali-treated duckweed biomass and duckweed-derived hydrothermal and pyrolytic biochar. *Environ. Sci. Pollut. Res.* 26(3), 2523-2530 (2019)
14. Philippou, K., Savva, I., Pashalidis, I.: Uranium(VI) binding by pine needles prior and after chemical modification. *Radioanal. Nucl. Ch.* 318, 2205–2211 (2018)
15. Hritcu, D., Humelnicu, D., Dodi, G., Popa M.I.: Magnetic chitosan composite particles: Evaluation of thorium and uranyl ion adsorption from aqueous solutions *Carbohydr. Polym.* 87, 1185– 1191 (2012)
16. Paschalidou, P., Liatsou, I., Pashalidis, I., Theocharis, C.R.: The effect of surface properties on the uranium adsorption by mesoporous ceria. *J. Radioanal. Nucl. Chem.* 318, 2193–2197 (2018)
17. Kutahyali, C., Eral, M.: Sorption studies of uranium and thorium on activated carbon prepared from olive stones: kinetic and thermodynamic aspects. *J. Nucl. Mater.* 396, 251-256 (2010)
18. Bhalara, P.D., Punetha, D., Balasubramanian, K.: Kinetic and isotherm analysis for selective thorium(IV) retrieval from aqueous environment using eco-friendly cellulose composite. *Int. J. Environ. Sci. Te.* 12, 3095-3106 (2015)
19. Riazi, M., Keshtkar, A.R., Moosavian, M.A.: Batch and continuous fixed-bed column biosorption of thorium(IV) from aqueous solutions: Equilibrium and dynamic modeling. *J. Radioanal. Nucl. Ch.* 301, 493-503 (2014)
20. Zhou, L., Wang, Y., Zou, H., Liang, X., Zeng, K., Liu, Z., Adesina, A.A.: Biosorption characteristics of uranium(VI) and thorium(IV) ions from aqueous solution using CaCl₂-modified Giant Kelp biomass. *J. Radioanal. Nucl. Ch.* 307, 635-644 (2016)
21. Li, Y., Wang, C., Guo, Z., Liu, C., Wu, W.: Sorption of thorium(IV) from aqueous solutions by graphene oxide. *J. Radioanal. Nucl. Chem.* 299, 1683-1691 (2014)

22. Pan, N., Deng, J., Guan, D., Jin, Y., Xia, C.: Adsorption characteristics of Th(IV) ions on reduced graphene oxide from aqueous solutions. *Appl. Surf. Sc.* 287, 478-483 (2013)